ORGANOMETALLICS

pubs.acs.org/Organometallics Article

# Ga(N,P) Growth on Si and Decomposition Studies of the N–P Precursor Di-*tert*-butylaminophosphane (DTBAP)

Johannes Glowatzki,*,§ Oliver Maßmeyer,*,§ Marcel Köster, Thilo Hepp, Ebunoluwa Odofin, Carsten von Hänisch, Wolfgang Stolz, and Kerstin Volz

Cite This: *Organometallics* 2020, 39, 1772–1781 Read Online

ACCESS | Metrics & More | Article Recommendations

**ABSTRACT:** III/V semiconductors containing small amounts of nitrogen (dilute nitrides) are promising for applications such as lasers and solar cells. Metal–organic vapor-phase epitaxy (MOVPE) is a widely used technique for growing III/V semiconductors on an industrial scale, and the growth of dilute nitrides with this method is promising for later successful market entry. The main issues of dilute nitrides are carbon incorporation and low nitrogen incorporation efficiency of the conventional N precursors. Due to the high N incorporation efficiency and the low decomposition temperature of the As and N precursor di-*tert*-butylaminoarsane (DTBAA), a similar P- and N-containing precursor, di-*tert*-butylaminophosphane (DTBAP), was synthesized and purified on a laboratory scale. Growth studies using this precursor were carried out in this work realizing Ga(N,P)/GaP multi quantum wells on Si and GaP substrates. The structures show evidence of N incorporation, and good layer structures were confirmed by high-resolution X-ray diffraction. Following the influence of different growth parameters on the N incorporation, the growth rate and surface morphology were characterized to set a foundation for possible growth applications in the future. DTBAP shows many advantages over the conventional N source 1,1-dimethylhydrazine (UDMHy) such as a much lower decomposition temperature of 310 °C and the realization of Ga(N,P) layers grown at temperatures as low as 475 °C with a high N incorporation of over 10%. Furthermore, the gas-phase decomposition of DTBAP has been studied with a real-time fast Fourier transform quadrupole ion trap mass spectrometer attached inline to the MOVPE reactor. The decomposition of DTBAP behaves very similarly to the As analogue DTBAA. On the one hand, the *tert*-butyl groups attached to DTBAP decompose radically, leading to the formation of isobutane, and decompose, on the other hand, by *β*-H elimination, leading to the formation of isobutene. Furthermore, the decomposition products indicate a direct cleavage of the P–N bond of the molecule, resulting in the formation of aminyl radicals ($NH_2^•$). The formation of $NH_2^•$ explains the high N incorporation efficiency of DTBAP at low temperatures as well as its limitations due to loss of $NH_3$ at higher temperatures.

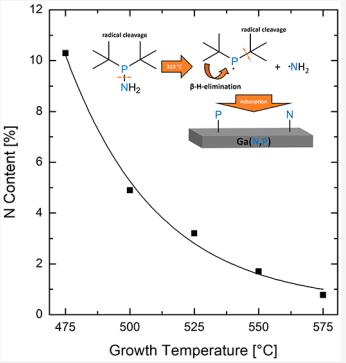




## 1. INTRODUCTION

GaP-based III/V semiconductors containing small amounts of nitrogen ("dilute nitrides") have been investigated because of their promising optoelectronic properties. The interaction of the nitrogen (N) level with the conduction band (band anticrossing model) leads to a strong reduction of the band gap energy.[1,2] The material system Ga(N,As,P) can be grown on silicon (Si) without relaxation and also shows direct band gap behavior.[3−5] It is a candidate for a monolithically integrated laser on Si. First optically and electrically pumped lasers were demonstrated on GaP and Si substrates, respectively.[6−8] This material class with different compositions is also a candidate for the top junction of a two-junction solar cell on Si.[9] Si as a substrate offers huge advantages in comparison to common III/V substrates. It is abundant, nontoxic, and well established in industry. In addition, solar cells, nanowires, and water-splitting solar cells were demonstrated with Ga(N,P).[10−13]

The GaP-based material systems have been grown with molecular beam epitaxy (MBE) and metal–organic vapor-phase epitaxy (MOVPE). For later realization of devices in mass production, MOVPE is a preferable method. Devices such as lasers and LEDs are produced these days with this method because of good scalability and high production output.[14] The disadvantages of MOVPE and the metal–organic precursors are the unintentional incorporation of impurities of alkyl groups and the restriction of growth temperatures because of the necessary thermal decomposition of the precursor. Large alkyl groups such as propyl and butyl groups are preferable because carbon (C) incorporation is probably more unlikely due to steric hindrance and the higher stability of the forming radicals in comparison to methyl

Received: February 5, 2020
Published: April 30, 2020




https://dx.doi.org/10.1021/acs.organomet.0c00078
*Organometallics* 2020, 39, 1772–1781

groups. However they also reduce the vapor pressure of the precursor. For the growth of dilute nitrides the nitrogen incorporation with the conventional precursor 1,1-dimethylhydrazine (UDMHy) is low and precursors with higher N incorporation efficiency are desirable.[15]

A novel arsenic (As)- and N-containing precursor (di-*tert*-butylaminoarsane, DTBAA) for the growth of GaAs-based dilute nitrides was investigated in the last few years and showed a high N incorporation in Ga(N,As), (Ga,In)(N,As), and Ga(N,As,Sb) and a low decomposition temperature.[16−19] On the basis of the experience with this precursor a similar N- and phosphorus (P)-containing precursor (di-*tert*-butylaminophosphane, DTBAP) was synthesized and tested in the function of a precursor for MOVPE.

To get further insight into the N incorporation of the novel precursor its thermal decomposition has been studied. Like the As analogue DTBAA DTBAP exhibits a N−group V bond instead of a direct C−N bond and the C is only present in large alkyl groups. Due to prevention of the strong C−N bond and steric restriction of the large alkyl groups it is expected that C incorporation will be reduced in the growing layers using these novel precursors.[20] In this regard the precursors should have an advantage in comparison to the commonly used N precursor 1,1-dimethylhydrazine (UDMHy). UDMHy exhibits strong N−N and C−N bonds as well as small alkyl groups. As shown in former decomposition studies, this leads to formation of $CH_4$, $N_2$, and larger stable fragments such as $(CH_3)_2NH$ and $CH_3NCH_2$ upon decomposition.[21] These fragments probably lead to comparably high C incorporation and low N incorporation efficiencies due to the high bond strength, especially for use at low growth temperatures.

In the following the synthesis, growth, and mass spectrometer results of the novel precursor DTBAP are presented. In the beginning N incorporation in GaP on Si substrates will be demonstrated and systematic investigations of the dependence on growth temperature and triethylgallium (TEGa), *tert*-butylphosphane (TBP), and DTBAP partial pressures will be shown. Subsequently the growth on GaP will be demonstrated and compared to the growth on Si. Finally, thermal decomposition studies of DTBAP via mass spectrometry will be shown.

## 2. SYNTHESIS OF $t$Bu$_2$PNH$_2$ (DTBAP)

An early synthesis of $t$Bu$_2$PNH$_2$ was performed by Scherer and Schieder in 1968.[22] In a first reaction of the Grignard reagent $t$BuMgCl with $PCl_3$ the compound $t$Bu$_2$PCl was prepared. This reactant was aminated with gaseous ammonia to give the desired product $t$Bu$_2$PNH$_2$.[22] The synthesis is sketched in Scheme 1.

**2.1. General Considerations.** All working procedures were conducted under rigorous exclusion of oxygen and moisture using a Schlenk line and nitrogen/argon atmosphere. Solvents were dried and freshly distilled before use. The starting materials $t$BuCl and $PCl_3$ were purchased from Acros Organics, and magnesium was obtained from Sigma-Aldrich. NMR (nuclear magnetic resonance) spectra were recorded on a Bruker AvanceHD 300 instrument with the following multiplicities: s = singlet, d = doublet.

**Scheme 1. Synthesis of $t$Bu$_2$PNH$_2$ (DTBAP)**

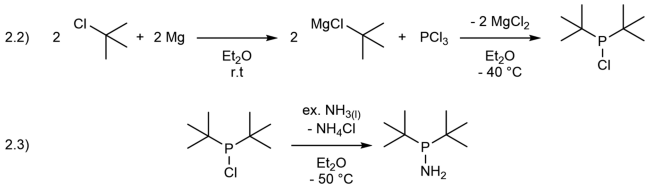


**2.2. $t$Bu$_2$PCl.** A solution of $t$BuCl (55.1 mL, 0.50 mol, 2.5 equiv) and 150 mL of diethyl ether was added dropwise to a suspension of magnesium (12.2 g, 0.50 mol, 2.5 equiv) and 200 mL of diethyl ether at room temperature. This Grignard solution was then added dropwise to a solution of $PCl_3$ (17.5 mL, 0.20 mol, 1.0 equiv) in 400 mL of diethyl ether at −40 °C. After the mixture was warmed to rt, the formed precipitate was filtered and washed twice with 40 mL portions of *n*-pentane. Removal of the solvent *in vacuo* provided the raw product as a colorless liquid which was purified via fractional distillation at 10 mmHg at 63 °C (18.0 g, 0.10 mol, 50% yield). $^1$H NMR (300.13 MHz, $C_6D_6$): $\delta$/ppm 1.09 [d, $^3J_{HP}$ = 12.1 Hz, 18H, $CH_3$]. $^{13}C\{^1H\}$-NMR (75.47 MHz, $C_6D_6$): $\delta$/ppm 27.9 [d, $^2J_{CP}$ = 17.1 Hz, $CH_3$], 35.9 [d, $^1J_{CP}$ = 41.3 Hz, $C_{quart}$]. $^{31}P\{^1H\}$-NMR (121.54 MHz, $C_6D_6$): $\delta$/ppm 148.1 [s, *P*Cl].

**2.3. $t$Bu$_2$PNH$_2$.** Gaseous ammonia was passed through a solution of $t$Bu$_2$PCl (10 g, 0.55 mol, 1.0 equiv) and 10 mL of diethyl ether for 1 h at −50 °C. The resulting precipitate was filtered after it was warmed to rt and washed twice with 10 mL portions of *n*-pentane. Removal of the solvent *in vacuo* provided the raw product as a colorless liquid which was purified via fractional distillation at 5 mmHg and 55 °C (8.06 g, 0.50 mol, 90% yield). $^1$H NMR (300.13 MHz, $C_6D_6$): $\delta$/ppm 0.92 [s, 2H, N*H*], 1.03 [d, $^3J_{H,P}$ = 11.2 Hz, 18H, $CH_3$]. $^{13}C\{^1H\}$-NMR (75.47 MHz, $C_6D_6$): $\delta$/ppm 28.1 [d, $^2J_{C,P}$ = 15.4 Hz, $CH_3$], 33.0 [d, $^1J_{C,P}$ = 21.5 Hz, $C_{quart}$]. $^{31}P\{^1H\}$-NMR (121.54 MHz, $C_6D_6$): $\delta$/ppm 63.0 [s, *P*$NH_2$].

## 3. GROWTH AND CHARACTERIZATION OF Ga(N,P)-CONTAINING SAMPLES

All samples were grown using MOVPE. An AIXTRON AIX 200 reactor system with gas foil rotation was used. The reactor pressure was held at 50 mbar under a total gas flow of 6800 sccm for all experiments. Palladium cell purified hydrogen (purity: 9.0) was used as the carrier gas. *tert*-Butylphosphane (TBP), triethylgallium (TEGa), and DTBAP were used as precursors. The vapor pressure of the novel precursor DTBAP was unknown at the beginning of the experiments and was estimated via consumption calculations afterward to be around 1 mbar at 20 °C. The samples were grown either on exact semiinsulating Si (001) substrates with a 28 nm GaP nucleation on top or on exact semiinsulating GaP (001) substrates. For a high-quality surface both substrates were processed with a pretreatment. The GaP/Si substrate was heated (unstabilized and TBP stabilized) and a thin 12 nm GaP buffer was grown under optimized conditions at 675 °C. A thicker buffer was not possible because of relaxation at large GaP thickness. The GaP substrate was processed with different etching steps before pretreatment in the reactor. The samples were heated and afterward overgrown with a 250 nm thick GaP buffer. Test structures were grown to determine the N incorporation as three times multi quantum wells (MQWs) at temperatures between 475 and 575 °C. Cooling after buffer growth was done under TBP stabilization to prevent P desorption. Between 7 and 21 nm thick Ga(N,P) QWs and thin 7−11 nm GaP barriers were grown. Thicker barriers were avoided to prevent the samples from relaxation. The structure


https://dx.doi.org/10.1021/acs.organomet.0c00078
Organometallics 2020, 39, 1772−1781

was always finished with a QW and cooled to 350 °C under TBP stabilization to determine the surface morphology realistically. The TEGa, DTBAP, and TBP partial pressures and also the growth temperature were varied systematically and the influence on the N incorporation, growth rate, and surface morphology were investigated.

The surface morphology of the samples was investigated using a Nanoscope IIIa atomic force microscopy (AFM) setup from Digital Instruments. The AFM images shown have a size of 5 × 5 $\mu$m.

The structure of the samples was investigated using a Panalytical X'Pert Pro high-resolution X-ray diffraction (HRXRD) system with a Cu anode monochromated to the Cu $K_\alpha$ line (wavelength of 0.15405 nm). By measurements around the substrate (Si or GaP) (004) reflection and dynamic simulations of the diffractograms with the X'Pert Epitaxy smooth and fit software the N content and growth rate of the Ga(N,P) layers could be determined. At different times during the experiments, samples with nominally the same growth conditions were prepared to ensure reproducibility and obtain the error for different growth runs. The growth conditions were as follows: $T_{gr}$ = 525 °C, $P_p$(TBP) = 0 mbar, $P_p$(TEGa) = 7.1 × $10^{-3}$ mbar, and $P_p$(DTBAP) = 1.8 × $10^{-2}$ mbar. The average N content of these samples is 2.12% with a standard deviation of 0.13%. As this value is larger than the estimated error from the simulations, this value is taken as the error for the compositions. For the growth rate the estimated error of the simulations leads to an error of 0.01 nm/s for the growth rate, if not noted differently.

## 4. MASS SPECTROMETER MEASUREMENTS OF DTBAP

To study the thermal decomposition of DTBAP, a quadrupole ion trap mass spectrometer from Carl Zeiss GmbH (iTrap) was used in line with the MOVPE system. The setup is designed to achieve measurement conditions as close to realistic growth conditions as possible and has been successfully used for gas-phase investigations of *tert*-butylarsane (TBAs) and DTBAA before.[16,23] The ion trap uses standard electron impact ionization with 70 eV for ion generation. The ions were then captured by an oscillating electric field applied to the ring electrode of the ion trap. The frequency of the oscillation used is within the radio frequency (RF) range. The mass range of interest can be selected by the adjustment of the applied RF voltage, which changes the strength of the electric field. Due to the oscillations of the ions within the trap an induced mirror image current within the top and bottom electrodes of the trap can be measured. This current signal was then analyzed by fast Fourier transformation, which enabled recording times for a single mass spectrum below 2 s. Therefore, the setup is suitable for real time analysis during the MOVPE process and the fast measurement times allow high data point densities and good statistics. Generally, quadrupole ion traps offer high sensitivity leading to detection of impurities in the parts per trillion concentration level with this setup.[24]

Due to the setup, the precise measurement of the gas-phase temperature at the point of gas collection was not possible and only the surface temperature of the susceptor was measured. By correlation of TBAs decomposition curves from ref 23 with data taken from ref 25 the gas-phase temperature was determined.

## 5. RESULTS AND DISCUSSION

The following part is organized as follows. In the beginning the first evidence of nitrogen incorporation in GaP on the Si substrate will be shown and experiments with varying growth conditions will follow. Furthermore, Ga(N,P) growth on GaP substrates will be shown and compared to growth on Si substrates. Finally mass spectrometer measurements and decomposition curves of the DTBAP will be shown.

**5.1. MOVPE Growth Experiments on Si.** The first evidence of Ga(N,P) growth including sufficient nitrogen incorporation using DTBAP was obtained with HRXRD for all investigated samples.

As an example, the HRXRD diffractogram and dynamic simulation of one sample grown with a partial pressure of DTBAP of 1.8 × $10^{-2}$ mbar and a TEGa partial pressure of 7.1 × $10^{-3}$ mbar without TBP at a growth temperature of 525 °C are shown in Figure 1.

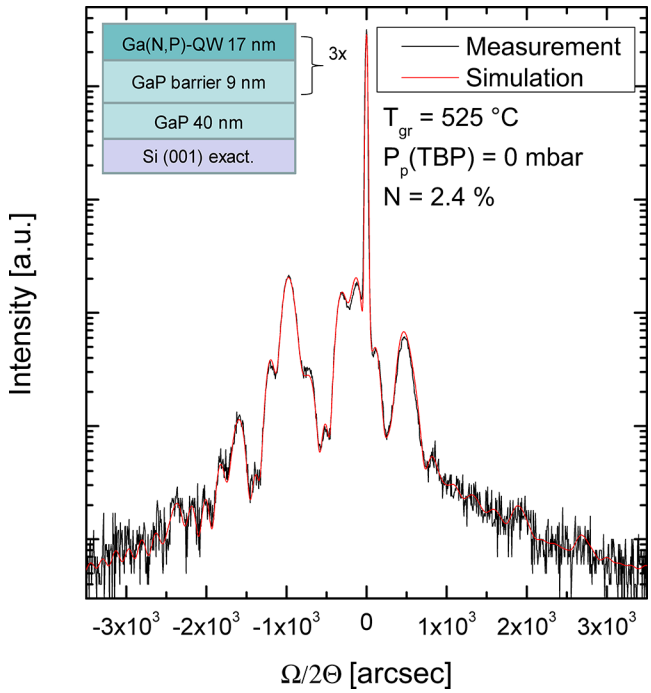


**Figure 1.** Example of an HRXRD diffractogram of a Ga(N,P)/GaP multiquantum well on Si with dynamic simulation.

Simulation and measurement are in good agreement, and all fringes are resolved well, which indicates high-quality layers. If not noted otherwise, all samples show good HRXRD measurements. Thus, in the following only the N content and growth rate are plotted.

In Figure 2 the N incorporation and the growth rate are plotted versus the TBP partial pressure for two different DTBAP partial pressures. For all samples the TEGa partial pressure as well as the growth temperature were kept constant (7.1 × $10^{-3}$ mbar and 525 °C, respectively). An additional supply of TBP during growth reduces the N incorporation. The highest N incorporation was obtained using no TBP and a higher DTBAP partial pressure, while the N incorporation was reduced for lower DTBAP partial pressure and no TBP. This also means that no additional P source is needed and DTBAP delivers both elements N and P simultaneously. This behavior was also seen for the As analogue DTBAA. In this case


https://dx.doi.org/10.1021/acs.organomet.0c00078
Organometallics 2020, 39, 1772−1781

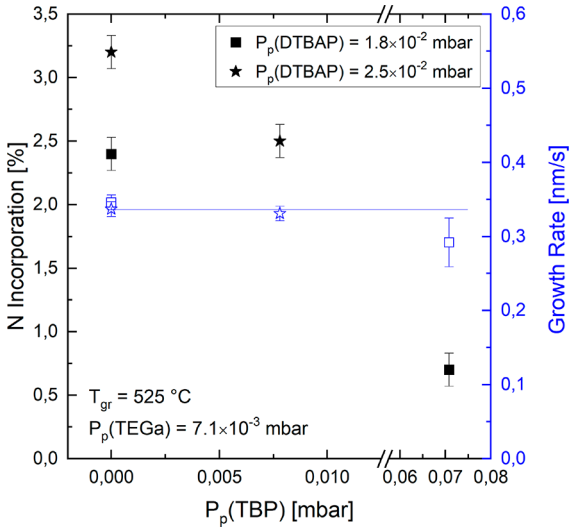


**Figure 2.** N incorporation and growth rate in dependence of the TBP partial pressure. DTBAP and TEGa partial pressures and growth temperature were kept constant.

Ga(N,As) layers on GaAs were realized without an additional As source.[19]

The N incorporation is low compared to the P incorporation, which means that P is much more efficiently incorporated. This can be related to the metastability of Ga(N,P) grown on GaP. Under equilibrium conditions the solubility of N in GaP is in the parts per million level. Only due to the growth far from equilibrium can N incorporation in GaP be realized, as is done in MOVPE.[26,27] Also additional P from the TBP is competing for the group V lattice sites and further reduces the N incorporation. The N/P ratio seems to be crucial for the N incorporation, as is also seen for growth studies of Ga(N,P) with UDMHy and for the growth of Ga(N,As) with the As analogue DTBAA.[15,19] The TBP partial pressure has no influence on the growth rate, since the group III supply should be growth-limiting under these conditions. This means also that the effective V/III ratio is larger than 1.

Since there is no need to add TBP and the highest N incorporation was reached without TBP, further experiments were carried out without TBP. The DTBAP partial pressure was varied systematically at a growth temperature of 525 °C while TEGa partial pressure was kept constant ($7.1 \times 10^{-3}$ mbar). The results of this experiment are shown in Figure 3a.

Increasing the DTBAP partial pressure increases the N incorporation linearly. There are many reasons this dependence could happen. As was mentioned before, the N/P ratio seems to be crucial for N incorporation but the N/P ratio is fixed to unity in the molecule itself. However, gas-phase reactions in combination with surface and catalytic reactions could lead to varying N/P ratios dependent on the DTBAP partial pressure and the (N + P)/Ga ratio. One can also consider the influence of the surface reconstruction, which may change depending on the (N + P)/Ga ratio. A change of the surface reconstruction on the V/III ratio has been widely studied for GaAs (001) surfaces and is also seen for GaP (001) surfaces.[28−31] Even an increase in the N incorporation on more Ga rich surfaces has been seen for Ga(N,As) grown in GaAs as well as has been predicted for Ga(N,P).[32,33] The complete mechanism behind this incorporation behavior remains unclear and has to be investigated in the future in more detail.

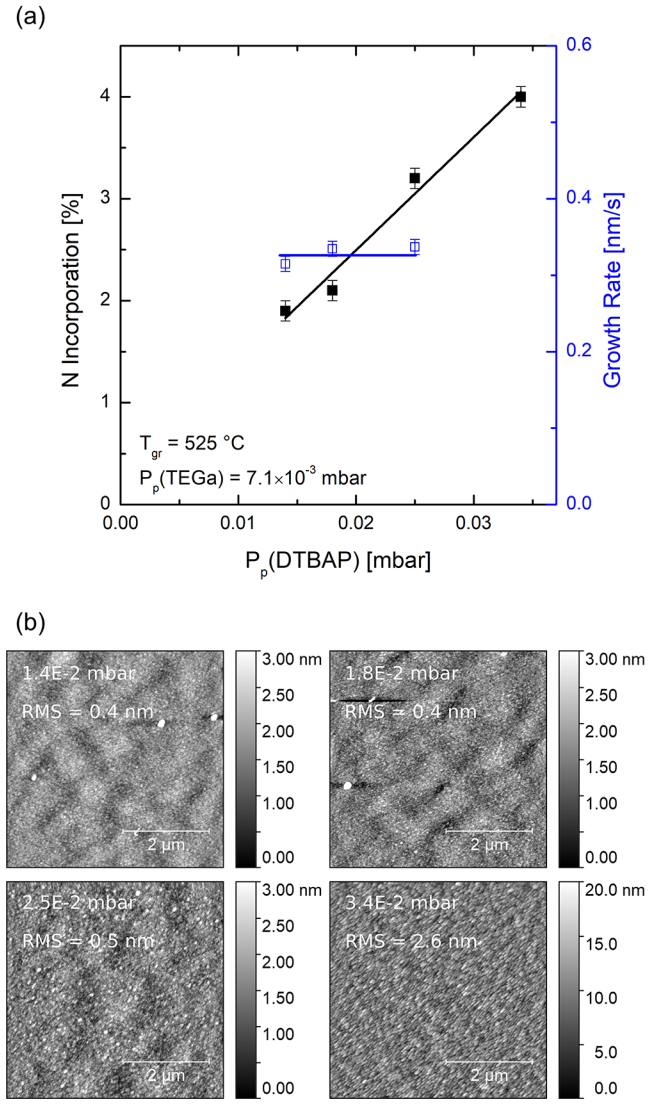


**Figure 3.** (a) N incorporation and growth rate dependence on the DTBAP partial pressure. The TEGa partial pressure and growth temperature were kept constant, and no TBP was added. (b) AFM images (size 5 × 5 $\mu$m) of some samples from (a). DTBAP partial pressures and RMS values are given as insets.

Furthermore, the growth rate does not seem to change, which is expected because of the same reasons mentioned before in the discussion of Figure 2. AFM images from the surfaces of the samples grown with different DTBAP partial pressures are shown in Figure 3b. At lower amounts of DTBAP the surfaces are flat and show a small roughness but there are some larger three-dimensional (3D) structures on it. Most likely these are Ga droplets occurring because of a low effective (N + P)/Ga ratio. The sample grown with $P_p$(DTBAP) = $2.5 \times 10^{-2}$ mbar is smooth without 3D features but is rougher than the surfaces mentioned before. A higher $P_p$(DTBAP) leads to a very rough surface with 3D islandlike structures. In addition, the HRXRD measurement of this sample showed a single Ga(N,P) layer instead of a three times multi quantum well structure. Probably due to high strain the growth mode changed and only highly defective layers were deposited after a specific thickness.

Further the TEGa partial pressure was varied systematically at a growth temperature of 525 °C and a fixed DTBAP partial pressure of $1.8 \times 10^{-2}$ mbar. The N incorporation and growth


https://dx.doi.org/10.1021/acs.organomet.0c00078
Organometallics 2020, 39, 1772−1781

rate are plotted in Figure 4. With increasing TEGa partial pressure the N incorporation decreased and the last data point

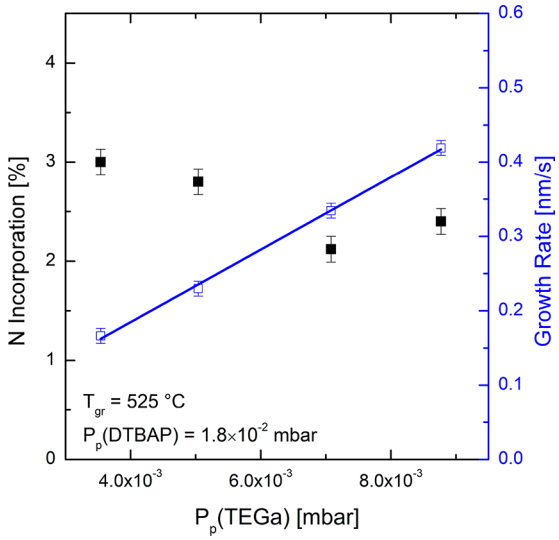


**Figure 4.** N incorporation and growth rate dependent on the TEGa partial pressure. The DTBAP partial pressure and growth temperature were kept constant, and no TBP was added.

remained constant within the error or even increased again. Possible explanations for the decreasing N content could be most likely the lowering of the (N + P)/Ga ratio that resulted in a lower N incorporation as seen in Figure 3a. In addition a constant sticking coefficient at a certain temperature of the active N species could explain this behavior, since by increasing the growth rate less N can be incorporated due to the shorter period of time per monolayer growth.

The increased N incorporation at higher TEGa partial pressures perhaps originates from a change in the surface reconstruction at low V/III ratios. At low V/III ratios the surface can change to a more Ga rich surface reconstruction.[30,31] For these more Ga rich surfaces an enhanced N incorporation has been predicted in the literature and some evidence for this has been seen for growth of Ga(N,As) on GaAs (001) surfaces.[32,33] The growth rate is increasing proportionally to the TEGa partial pressure due to the growth-limiting character of the group III supply in the group V rich growth regime.

While the gas phase composition was kept constant, the growth temperature was changed systematically. The DTBAP and the TEGa partial pressures were kept constant at 2.5 × $10^{-2}$ mbar and 7.1 × $10^{-3}$ mbar, respectively. In Figure 5a the N content and the growth rate are plotted versus the growth temperature. The N incorporation is increasing exponentially (exponential behavior is discussed later in section 5.3) with a decrease in the growth temperature, and a N content of about 10% was reached at a growth temperature of 475 °C. Growth with this amount of N at this low temperature has not been reported for MOVPE growth with the conventional N precursor UDMHy.[15] By further optimization of the growth conditions even higher N contents should be realizable, which could compete with N fractions of up to 16% realized in Ga(N,P) layers grown by MBE.[34] This exponential behavior of the N incorporation implies a thermally activated loss process with an activation energy, which will be shown in section 5.3. One can think of loss processes such as desorption of the active

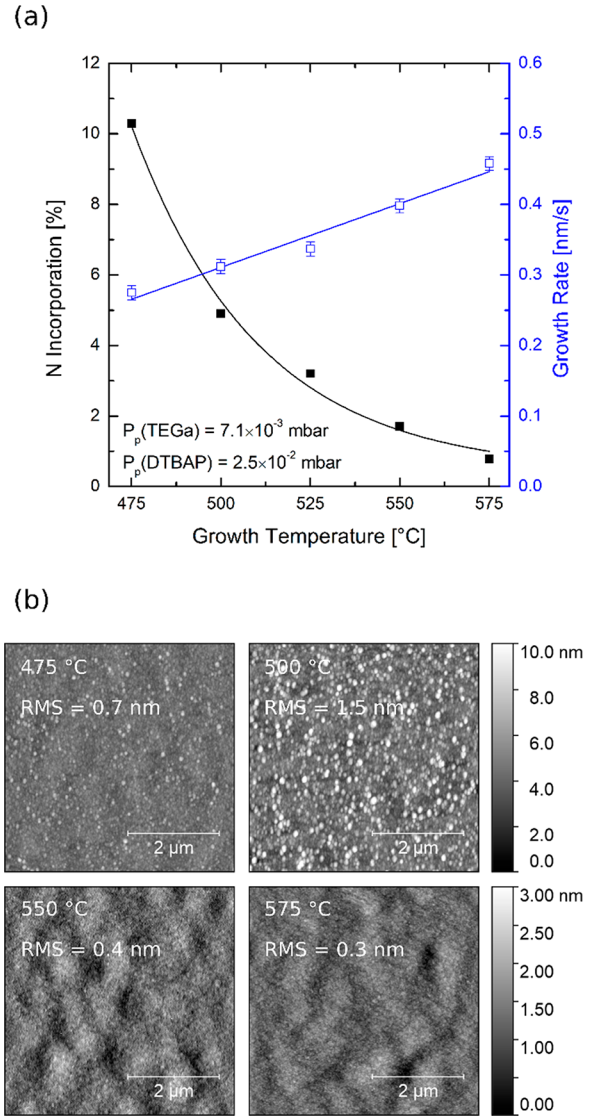


**Figure 5.** (a) N incorporation and growth rate dependent on the growth temperature. TEGa and DTBAP partial pressures were kept constant, and no TBP was added. (b) AFM images (size 5 × 5) of some samples from (a). Temperature and RMS values are given as insets.

nitrogen species from the surface or a loss due to gas-phase reactions of the active species to more stable products, which are not incorporated efficiently. This idea is supported by formation of aminyl radicals ($NH_2^•$) that form upon decomposition. $NH_2^•$ is likely to form $NH_3$, which could prevent N incorporation at higher temperatures and will be discussed in section 5.3. The growth rate is increasing linearly with the growth temperature. Possibly there is a larger supply of the growth-limiting group III species due to a higher diffusion rate from the boundary layer to the surface. Higher decomposition of the Ga precursor should not be the reason, since the decomposition temperature in our reactor is measured as 250 °C, which is in agreement with the literature data for TEGa.[35,36] The desorption of surface-blocking alkyl groups could also explain the increase in growth rate. The site blocking seems to be the most likely explanation, since it has been studied in different growth experiments with MOVPE.[37−39] In Figure 5b 5 × 5 μm AFM images of the


https://dx.doi.org/10.1021/acs.organomet.0c00078
Organometallics 2020, 39, 1772−1781

surfaces from samples grown at different temperatures are shown. For higher temperatures the surfaces do not show steps or an otherwise distinct morphology but they are smooth with wavylike modulation in the micrometer lateral range. The wavylike modulation can be directly related to nucleation of the GaP on the Si substrate, as it is not seen on GaP substrates. This will be shown in section 5.2. For lower growth temperatures, the surfaces are rougher and show 3D features on top and the underlying surfaces are looking similarly smooth as the samples grown at higher temperatures. Roughening of the surface and 3D island formation could be related to the higher N content and the lower diffusion rate on the surface with decreased temperature. In addition samples of the TEGa and DTBAP partial pressure series, which are discussed in Figure 3a, showed rougher surfaces and similar (but smaller) 3D features for higher N contents. It is remarkable that the surface got smoother and showed fewer 3D features for the lowest growth temperature with the highest amount of N. Probably the formation of these 3D features is related to the strain induced by the high N content and the high miscibility gap in this metastable material system. Additionally, an activation energy should be necessary for the change in growth mode from 2D to 3D growth which occurs at higher temperatures. Thus, the formation seems to be both temperature as well as strain induced.

**5.2. MOVPE Growth Experiments on GaP.** In addition to the growth experiments on GaP/Si, a few samples were grown under similar growth conditions on GaP substrates for comparison. AFM images (size 5 x 5 $\mu$m) of samples grown under same conditions on GaP/Si and GaP substrates are shown in Figure 6.

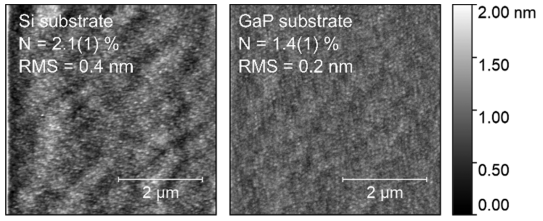


**Figure 6.** AFM images (size 5 x 5 $\mu$m) of samples grown under the same growth conditions but on different substrates (Si vs GaP). The growth conditions are $P_p$(TEGa) = 7.1 × $10^{-3}$ mbar, $P_p$(DTBAP) = 2.5 × $10^{-2}$ mbar, and $T_g$ = 525 °C. In the AFM images the N incorporation and the RMS values are shown.

The surfaces look very similar, but the sample grown on GaP/Si shows a wavylike modulation in the micrometer lateral range as mentioned above and the sample grown on GaP does not show these modulations. This implies that these modulations occur due to the growth on Si. The N incorporation of 2.1 ± 0.1% in layers grown on GaP/Si is significantly higher than that on GaP (1.4 ± 0.1%). In general, the effects of lattice pulling and lattice latching have been described in the literature and can describe the observed incorporation effect. The epitaxial growth of thin layers with a lattice constant different from that of the substrate introduces a strain energy due to lattice deformation, which increases the total free energy of the system. One way to reduce the total free energy is a change in the alloy composition and, therefore, a change in lattice constant and mismatch.[39] For the material system (Ga,In)P the effect of lattice mismatch on the composition of the solid was investigated in 1972 for the liquid-phase epitaxy method.[40] Lattice pulling effects were also seen in the MOVPE growth of (Ga,In)N on GaN and also for the dilute nitride material system (Ga,In)(N,As) on (Ga,In)-As.[41,42] An effect of lattice mismatch on solid composition was also seen for MOVPE grown Ga(N,As) on GaP. In contrast to the growth on GaAs the N incorporation was improved drastically by a factor of about 10. This was explained by the compressive strain of Ga(N,As) on GaP up to a fraction of 17.8% N which results in strain compensation. In contrast N incorporation results in tensile strain over the whole composition window for Ga(N,As)/GaAs.[43] In this study the compressive strain of Ga(N,P) on Si up to a N content of around 2% also leads to the lattice pulling effect and allows a higher incorporation due to the strain-compensating effect of N at these compositions. This is in contrast to the growth on GaP, where N incorporation introduces tensile strain for every composition.

**5.3. Decomposition Studies via Mass Spectrometry.** To provide a deeper insight into the N incorporation behavior into Ga(N,P), the thermal decomposition of DTBAP (161 u) has been investigated with an ion trap connected to the MOVPE system. The detected mass spectrum at a temperature of 50 °C for a supplied partial pressure of 3 × $10^{-3}$ mbar is shown in Figure 7a. For comparison the detected intensities

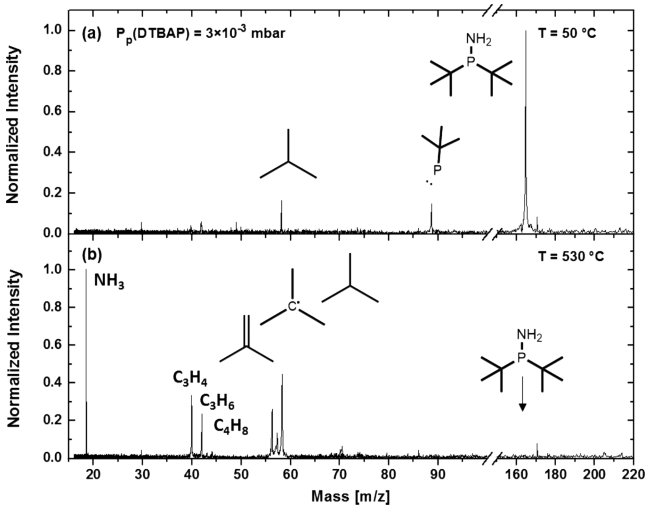


**Figure 7.** Detected mass spectra of DTBAP (161 u) at different temperatures for a partial pressure of 3 × $10^{-3}$ mbar. (a) Electron-induced fragmentation of DTBAP at 50 °C. Due to a comparably low filament current of 1.3 A and a short time between the gas inlet and the ionization with 70 eV, only a few fragments with low intensity are detected. (b) Decomposition spectrum of DTBAP at 530 °C. Mainly isobutane (58 u), *tert*-butyl radicals (57 u), isobutene (56 u), and $NH_3$ (17 u) are detected. The detected carbon chains at 40, 42, and 44 u can be attributed to electron-induced fragmentation of isobutane and isobutene.

are normalized to the signal of DTBAP at 161 u. At this temperature no decomposition occurs and all fragmentation products within this figure are induced by electron impact ionization. Using optimized parameters within the ion trap, the electron-induced fragmentation is reduced to a minimum. Therefore, most DTBAP molecules are not fragmented by the electrons and only a few fragments such as isobutane (58 u) and probably $C_4H_9P^{\bullet\bullet}$ (88 u) are visible. This simplifies the interpretation of the DTBAP decomposition.


https://dx.doi.org/10.1021/acs.organomet.0c00078
Organometallics 2020, 39, 1772−1781

The thermally induced decomposition of DTBAP at a temperature of 530 °C can be seen in Figure 1b. The intensity of DTBAP completely vanishes at this temperature, indicating complete decomposition of the DTBAP. As fragments mainly isobutane (58 u), *tert*-butyl radicals (57 u), isobutene (56 u), and $NH_3$ (17 u) are detected. These can all be attributed to thermal decomposition. Isobutane and *tert*-butyl radicals are the products of radical decomposition of the C−P bond within the molecule. This radical cleavage leads to the formation of *tert*-butyl radicals that can react with available H radicals or $H_2$ to form isobutane. Furthermore, there is the possibility of an intramolecular coupling reaction of the *tert*-butyl group with an H atom of the aminyl group, resulting in formation of isobutane. These reaction pathways have been predicted by density functional theory calculations for the As analogue DTBAA and are on the one hand shown in decomposition studies of this precursor. On the other hand these pathways are also known for other metal−organic precursors with *tert*-butyl groups such as TBAs.[16,25,44] Another expected reaction pathway of the *tert*-butyl groups is decomposition through *β*-H elimination. In this case a H atom at one of the C atoms in a *β* position within the *tert*-butyl group interacts with the p orbitals of the phosphorus atom of the same molecule. This leads to the formation of a C═C double bond (formation of isobutene) and a PH group. The corresponding reaction scheme can be found in ref 16 for the DTBAA molecule. *β*-H elimination seems to be a relevant decomposition pathway of at least one of the *tert*-butyl groups of the DTBAP, since isobutene was detected within the same magnitude as that for the *tert*-butyl radicals and the isobutane.

In the decomposition spectrum also lighter alkyl groups are visible. From former investigations of appropriate test gases, the intensities of the smaller alkyl chains around 42 and 40 u can be attributed to electron-induced fragmentation of isobutane and isobutene. The test gases have been investigated under the same ion trap settings and showed formation of propene (42 u) and propyne (40 u) in the case of isobutane and formation of propyne (40 u) for isobutene.

Additionally, $NH_3$ was detected with the same intensity as that for DTBAP. The detected $NH_3$ is attributed to the formation of aminyl radicals ($NH_2^\bullet$ 16 u) during the decomposition of DTBAP and was also observed as a decomposition product of DTBAA.[16] This indicates a radical decomposition of the N−P bond of the molecule, which leads to the formation of $NH_2^\bullet$ and DTBP$^\bullet$ (145 u). No evidence for DTBP$^\bullet$ has been found within this measurement, but the As analogue DTBA$^\bullet$ has been detected in the case of DTBAA. Therefore, it is expected that the DTBP$^\bullet$ fragments are either less stable or more reactive in comparison to DTBA$^\bullet$ in the decomposition of DTBAA. Either this is caused by dissociation into isobutane, *tert*-butyl radicals, isobutene and P or the DTBP$^\bullet$ adsorbs first to an available surface before dissociation and is therefore not detectable within the ion trap. No further fragments containing P have been measured. Any elemental P arising from the reaction would react to give $P_2$ or $P_4$, which is seen as a coating of the liner in the reactor. The $NH_2^\bullet$ radicals formed explain to some extent the N incorporation behavior seen in Figure 5a. At high temperatures $NH_2^\bullet$ is very likely to form $NH_3$ in the presence of $H_2$ or H$^\bullet$ and can therefore easily desorb from the growth surface or be generated in the gas phase. For low temperatures $NH_2^\bullet$ radicals are more likely to stick to the surface, leading to the efficient incorporation of N. These considerations lead to the predicted decomposition pathway for P incorporation shown in Scheme 2. The aminyl radicals are expected to be incorporated at low temperatures.

**Scheme 2. Proposed Reaction Pathway**

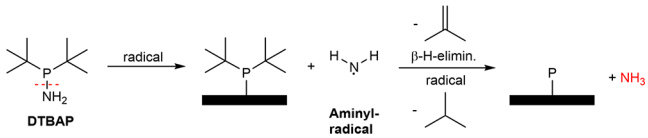


The temperature-dependent decomposition of DTBAP is shown in Figure 8. All major decomposition products

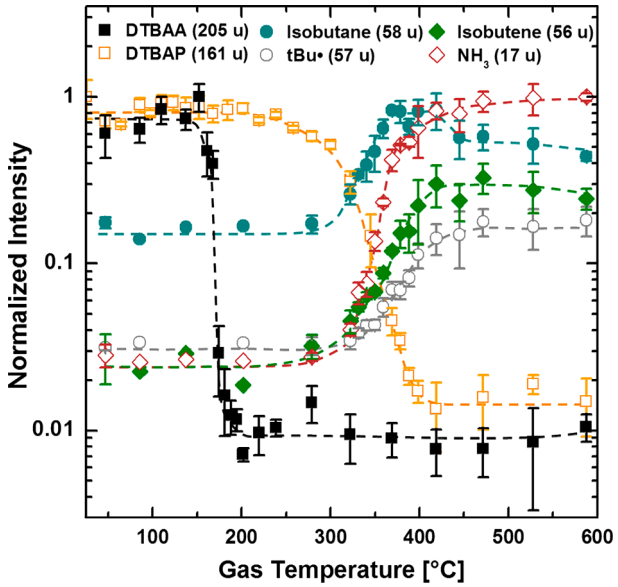


**Figure 8.** Decomposition curves of DTBAP (161 u) and DTBAA (205 u) for partial pressures of $3 \times 10^{-3}$ mbar and $2.5 \times 10^{-3}$ mbar, respectively. The most relevant decomposition fragments isobutane (58 u), *tert*-butyl radicals (57 u), isobutene (56 u), and $NH_3$ (17 u) of the DTBAP decomposition are included. Data of DTBAA from ref 16 measured within the same reactor are included as a comparison.

discussed above are included. As a comparison the decomposition curve of the As analogue DTBAA is included from ref 16. In comparison to DTBAA ($T_{decomp}$ = 160 ± 10 °C) the DTBAP decomposes at a higher temperature of $T_{decomp}$ = 310 ± 10 °C, which is defined as the point where the DTBAP signal drops to half of its intensity. This change in decomposition temperature is known, for example, for precursors such as TBAs ($T_{decomp}$* = 350 ± 10 °C) in comparison to TBP ($T_{decomp}$* = 400 ± 10 °C). (Values marked by * measured within the same reactor system. These determined temperatures are 30−50 °C lower in comparison to values from refs 25 and 45. This might be caused by the different experimental setups, different surface areas within the experiment, or different temperature measurement.) Immediately as the DTBAP decomposes, the intensities of isobutane, *tert*-butyl radicals, isobutene and $NH_3$ are increasing. Regarding the decomposition of the *tert*-butyl groups the radical or intramolecular coupling reaction seems to be the most relevant pathway over the whole temperature range, since isobutane summed together with the *tert*-butyl radicals shows the highest intensities. Nevertheless, the isobutane signal drops again for higher temperatures of around 450 °C. This shows


https://dx.doi.org/10.1021/acs.organomet.0c00078
Organometallics 2020, 39, 1772−1781

similarly to the DTBAA decomposition that one of the radical pathways might be hindered and the $\beta$-H elimination reaction becomes more relevant above this temperature. This is shown by the isobutene intensity, which is still increasing, while the isobutane intensity is already constant and remains stable within the same magnitude at higher temperatures.

An Arrhenius plot of the DTBAP decomposition data from Figure 8 and the nitrogen incorporation data from Figure 5a is shown in Figure 9. From the linear regression one can extract

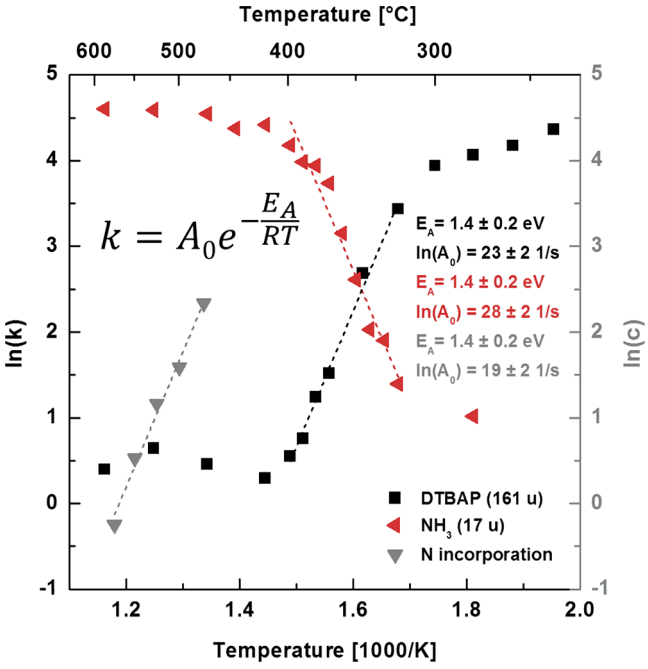


**Figure 9.** Arrhenius plot of the detected intensities of DTBAP and $NH_3$ together with the N concentration from Figure 5a. Activation energies and attempt frequency factors $A_0$ for the decomposition and N incorporation can be determined from the slope according to the Arrhenius equation shown in the inset.

the activation energies as well as the pre-exponential attempt frequency factors $A_0$. The activation energies of the DTBAP decomposition and the $NH_3$ production as well as the N incorporation are all determined with 1.4 ± 0.2 eV. The attempt frequency factors are 23 ± 2 1/s for DTBAP, 28 ± 2 1/s for $NH_3$, and 19 ± 2 1/s for the N incorporation, which are all within a similar frequency. Notably the agreement in activation energies supports the assumption, on the one hand, that the N−P bond breaks within the first step of the DTBAP decomposition, leading to the formation of the aminyl radicals ($NH_2^\bullet$) and, on the other hand, that the formation of the aminyl radicals ($NH_2^\bullet$) is directly related to the N incorporation. As mentioned above, at low temperatures $NH_2^\bullet$ is likely to stick to the growth surface, leading to N incorporation. At higher temperatures $NH_2^\bullet$ can react with available $H_2$ or $H^\bullet$ radicals to form $NH_3$, which is stable under these conditions. This could enhance the desorption rate of N from the surface or prevent the adsorption to the surface by formation within the gas phase. These findings could fully explain the exponential dependence of N incorporation in Ga(N,P) on the growth temperature discussed in Figure 5a.

## 6. SUMMARY

In this work the novel N and P precursor di-*tert*-butylaminophosphane (DTBAP) was introduced and the very first MOVPE growth experiments and gas-phase decomposition measurements were carried out. The first evidence of significant N incorporation in GaP on Si and GaP substrates, resulting in good structural quality samples, was shown. The growth parameters were varied systematically, and the influence on N incorporation, growth rate, and surface morphology were determined to create a foundation for further growth studies aiming toward device applications.

Offering the additional P precursor TBP leads to a lowering of N incorporation due to competition for group V lattice sites and a decreasing N/P ratio. Increasing the amount of TEGa leads to a linear increase in growth rate and for higher V/III ratios to a decrease in N incorporation.

As for the precursor DTBAA, an increasing partial pressure of DTBAP leads to a linear increase in N incorporation. Since the N/P ratio is fixed to unity within the molecule, this is unexpected on first sight. Some mechanisms were discussed, but this behavior has to be checked in future experiments to give a reliable answer.

Increasing the growth temperature leads to an exponential decrease of N incorporation in the grown Ga(N,P) samples. As possible reasons thermally activated loss processes of the active nitrogen species due to desorption or gas-phase reactions were discussed. These correlate to the formation of aminyl radicals found in the decomposition study of DTBAP. The observed linear increase in growth rate is most likely related to a partial surface blocking by adsorbed alkyl groups at low temperatures. Additionally, a N content of over 10% was confirmed with HRXRD for a growth temperature of 475 °C, which has not been realized for Ga(N,P) samples grown by MOVPE before. Nitrogen incorporation on the Si substrate was significantly higher than that on GaP, which is related to lattice-pulling effects caused by the strain compensation for growth on Si.

The decomposition temperature of DTBAP was determined with $T_{decomp}$ = 310 °C from the decomposition curve, which makes it suitable for low-temperature growth in MOVPE. The decomposition studies suggest for DTBAP the same reaction pathway as for DTBAA.[16] The *tert*-butyl groups either undergo radical and intramolecular coupling reactions leading to formation of isobutane and *tert*-butyl radicals or dissociate from the molecule by $\beta$-H elimination, which is detected by the appearance of isobutene. These larger alkyl groups, especially the stable isobutene, should lead to lower C incorporation into the growing layer in comparison to structures grown with UDMHy. Furthermore, the N−P bond of DTBAP decomposes radically under the formation of aminyl radicals ($NH_2^\bullet$). The $NH_2^\bullet$ radicals seem to be directly related to the N incorporation. This is shown by the activation energy of 1.35 eV for N incorporation from the growth studies, which is in agreement to the one obtained from $NH_2^\bullet$ formation during thermal decomposition. Therefore, $NH_2^\bullet$ should explain the high N incorporation at low temperatures due to adsorption of $NH_2^\bullet$. On the other hand, formation of $NH_3$ in the gas phase or at the surface leads to prevention of N incorporation at higher temperatures.


https://dx.doi.org/10.1021/acs.organomet.0c00078
Organometallics 2020, 39, 1772−1781

## AUTHOR INFORMATION


### Corresponding Authors

**Johannes Glowatzki** − *Material Sciences Center and Department of Physics, Philipps-Universität Marburg, 35032 Marburg, Germany;* orcid.org/0000-0002-8440-2271; Email: Johannes.Glowatzki@physik.uni-marburg.de

**Oliver Maßmeyer** − *Material Sciences Center and Department of Physics, Philipps-Universität Marburg, 35032 Marburg, Germany;* orcid.org/0000-0001-6101-5706; Email: Oliver.Maßmeyer@physik.uni-marburg.de

### Authors

**Marcel Köster** − *Material Sciences Center and Department of Chemistry, Philipps-Universität Marburg, 35032 Marburg, Germany*

**Thilo Hepp** − *Material Sciences Center and Department of Physics, Philipps-Universität Marburg, 35032 Marburg, Germany*

**Ebunoluwa Odofin** − *Material Sciences Center and Department of Physics, Philipps-Universität Marburg, 35032 Marburg, Germany*

**Carsten von Hänisch** − *Material Sciences Center and Department of Chemistry, Philipps-Universität Marburg, 35032 Marburg, Germany*

**Wolfgang Stolz** − *Material Sciences Center and Department of Physics, Philipps-Universität Marburg, 35032 Marburg, Germany*

**Kerstin Volz** − *Material Sciences Center and Department of Physics, Philipps-Universität Marburg, 35032 Marburg, Germany*

Complete contact information is available at: https://pubs.acs.org/10.1021/acs.organomet.0c00078

### Author Contributions

[§]J.G. and O.M. contributed equally.


### Notes

The authors declare no competing financial interest.

## ACKNOWLEDGMENTS

This work was supported by the German Research Foundation (GRK 1782: "Functionalization of Semiconductors"), and the support for the mass spectrometer (iTrap) was provided by Carl Zeiss SMT GmbH.

## ABBREVIATIONS

AFM, atomic force microscopy; dilute nitrides, III/V semiconductors containing small amounts of nitrogen; DTBA$^{\bullet}$, di-*tert*-butylarsane radical; DTBAA, di-*tert*-butylaminoarsane; DTBAP, di-*tert*-butylaminophosphane; DTBP$^{\bullet}$, di-*tert*-butylphosphane radical; HRXRD, high-resolution X-ray diffraction; LEDs, light-emitting diodes; MBE, molecular beam epitaxy; MOVPE, metal−organic vapor-phase epitaxy; MQWs, multi quantum wells; NH$^{\bullet}$, aminyl radical; NMR, nuclear magnetic resonance; QW, quantum well; RMS, root mean square; TBAs, *tert*-butylarsane; TBP, *tert*-butylphosphane; TEGa, triethylgallium; UDMHy, 1,1-dimethylhydrazine

## REFERENCES


(1) Wu, J.; Shan, W.; Walukiewicz, W. Band Anticrossing in Highly Mismatched III−V Semiconductor Alloys. *Semicond. Sci. Technol.* **2002**, *17*, 860−869.

(2) Shan, W.; Yu, K. M.; Walukiewicz, W.; Wu, J.; Ager, J. W.; Haller, E. E. Band Anticrossing in Dilute Nitrides. *J. Phys.: Condens. Matter* **2004**, *16* (31), S3355−S3372.

(3) Kunert, B.; Zinnkann, S.; Volz, K.; Stolz, W. Monolithic Integration of Ga(NAsP)/(BGa)P Multi-Quantum Well Structures on (0 0 1) Silicon Substrate by MOVPE. *J. Cryst. Growth* **2008**, *310* (23), 4776−4779.

(4) Kunert, B.; Volz, K.; Koch, J.; Stolz, W. Direct-Band-Gap Ga(NAsP)-Material System Pseudomorphically Grown on GaP Substrate. *Appl. Phys. Lett.* **2006**, *88* (18), 182108.

(5) Kunert, B.; Volz, K.; Nemeth, I.; Stolz, W. Luminescence Investigations of the GaP-Based Dilute Nitride Ga(NAsP) Material System. *J. Lumin.* **2006**, *121* (2), 361−364.

(6) Borck, S.; Chatterjee, S.; Kunert, B.; Volz, K.; Stolz, W.; Heber, J.; Rühle, W. W.; Gerhardt, N. C.; Hofmann, M. R. Lasing in Optically Pumped Ga(NAsP)/GaP Heterostructures. *Appl. Phys. Lett.* **2006**, *89* (3), 031102−3.

(7) Kunert, B.; Reinhard, S.; Koch, J.; Lampalzer, M.; Volz, K.; Stolz, W. First Demonstration of Electrical Injection Lasing in the Novel Dilute Nitride Ga(NAsP)/GaP-Material System. *Phys. Status Solidi C* **2006**, *3* (3), 614−618.

(8) Liebich, S.; Zimprich, M.; Beyer, A.; Lange, C.; Franzbach, D. J.; Chatterjee, S.; Hossain, N.; Sweeney, S. J.; Volz, K.; Kunert, B.; Stolz, W. Laser Operation of Ga(NAsP) Lattice-Matched to (001) Silicon Substrate. *Appl. Phys. Lett.* **2011**, *99* (7), 071109.

(9) Geisz, J. F.; Olson, J. M.; Friedman, D. J.; Jones, K. M.; Reedy, R. C.; Romero, M. J. Lattice-Matched GaNPAs-on-Silicon Tandem Solar Cells. *Conf. Rec. Thirty-first IEEE Photovolt. Spec. Conf.* **2005**, 695−698.

(10) Sukrittanon, S.; Liu, R.; Breeden, M. C.; Pan, J. L.; Jungjohann, K. L.; Tu, C. W.; Dayeh, S. A. Radial Direct Bandgap P-i-n GaNP Microwire Solar Cells with Enhanced Short Circuit Current. *J. Appl. Phys.* **2016**, *120* (5), 055702.

(11) Sukrittanon, S.; Kuang, Y. J.; Dobrovolsky, A.; Kang, W. M.; Jang, J. S.; Kim, B. J.; Chen, W. M.; Buyanova, I. A.; Tu, C. W. Growth and Characterization of Dilute Nitride GaNxP1−x Nanowires and GaNxP1−x/GaNyP1−y Core/Shell Nanowires on Si (111) by Gas Source Molecular Beam Epitaxy. *Appl. Phys. Lett.* **2014**, *105* (7), 072107.

(12) Sukrittanon, S.; Liu, R.; Ro, Y. G.; Pan, J. L.; Jungjohann, K. L.; Tu, C. W.; Dayeh, S. A. Enhanced Conversion Efficiency in Wide-Bandgap GaNP Solar Cells. *Appl. Phys. Lett.* **2015**, *107* (15), 153901.

(13) Kargar, A.; Sukrittanon, S.; Zhou, C.; Ro, Y. G.; Pan, X.; Dayeh, S. A.; Tu, C. W.; Jin, S. GaP/GaNP Heterojunctions for Efficient Solar-Driven Water Oxidation. *Small* **2017**, *13* (21), 1603574.

(14) Jürgensen, H. Large-Scale MOVPE Production Systems. *Microelectron. Eng.* **1992**, *18* (1−2), 119−148.

(15) Kunert, B.; Koch, J.; Torunski, T.; Volz, K.; Stolz, W. MOVPE Growth Experiments of the Novel (GaIn)(NP)/GaP Material System. *J. Cryst. Growth* **2004**, *272* (1−4), 753−759.

(16) Maßmeyer, O.; Inacker, S.; Hepp, T.; Glowatzki, J.; Nattermann, L.; Sterzer, E.; Ritter, C.; Von Hänisch, C.; Stolz, W.; Volz, K. Decomposition Mechanisms of Di-Tert-Butylaminoarsane (DTBAA). *Organometallics* **2019**, *38* (16), 3181−3186.

(17) Sterzer, E.; Ringler, B.; Nattermann, L.; Beyer, A.; von Hänisch, C.; Stolz, W.; Volz, K. (GaIn)(NAs) Growth Using Di-Tertiary-Butyl-Arsano-Amine (DTBAA). *J. Cryst. Growth* **2017**, *467*, 132−136.

(18) Sterzer, E.; Maßmeyer, O.; Nattermann, L.; Jandieri, K.; Gupta, S.; Beyer, A.; Ringler, B.; Von Hänisch, C.; Stolz, W.; Volz, K. 1 EV Ga(NAsSb) Grown by MOVPE Using Di- Tertiary -Butyl-Arsano-Amine (DTBAA). *AIP Adv.* **2018**, *8* (5), 055329.

(19) Sterzer, E.; Beyer, A.; Duschek, L.; Nattermann, L.; Ringler, B.; Leube, B.; Stegmüller, A.; Tonner, R.; Von Hänisch, C.; Stolz, W.; Volz, K. Efficient Nitrogen Incorporation in GaAs Using Novel Metal Organic As-N Precursor Di-Tertiary-Butyl-Arsano-Amine (DTBAA). *J. Cryst. Growth* **2016**, *439*, 19−27.

(20) Zanella, P.; Porchia, M.; Rossetto, G.; Brianese, N.; Ossola, F.; Williams, J. O. Organometallic Precursors in the Growth of Epitaxial

Thin Films of III-V Semiconductors by Metal-Organic Chemical Vapor Deposition (MOCVD). *Chem. Mater.* **1991**, *3* (2), 225−242.
(21) Lee, R. T.; Stringfellow, G. B. Pyrolysis of 1,1 Dimethylhydrazine for OMVPE Growth. *J. Electron. Mater.* **1999**, *28* (8), 963−969.
(22) Scherer, O. J.; Schieder, G. Metallorganische Aminophosphine Und Phosphinimine. *Chem. Ber.* **1968**, *101* (12), 4184−4198.
(23) Nattermann, L.; Maßmeyer, O.; Sterzer, E.; Derpmann, V.; Chung, H. Y.; Stolz, W.; Volz, K. An Experimental Approach for Real Time Mass Spectrometric CVD Gas Phase Investigations. *Sci. Rep.* **2018**, *8* (319), 1−7.
(24) Chung, H. Y.; Aliman, M.; Fedosenko, G.; Laue, A.; Reuter, R.; Derpmann, V.; Gorkhover, L.; Antoni, M. Very Sensitive Real-Time Inline Process Mass Spectrometer Based on FFT Ion Trap Technique. *Annu. SEMI Adv. Semicond. Manuf. Conf. ASMC 2016 27th* **2016**, 263−266.
(25) Larsen, C. A.; Buchan, N. I.; Li, S. H.; Stringfellow, G. B. Decomposition Mechanisms of Tertiarybutylarsine. *J. Cryst. Growth* **1989**, *94* (3), 663−672.
(26) Stringfellow, G. B. Calculation of the Solubility and Solid-Gas Distribution Coefficient of N in GaP. *J. Electrochem. Soc.* **1972**, *119* (12), 1780−1782.
(27) Kaprinski, J.; Jun, J.; Grzegory, I.; Bugajski, M. Crystal Growth of GaP Doped with Nitrogen under High Nitrogen Pressure. *J. Cryst. Growth* **1985**, *72* (3), 711−716.
(28) Ohtake, A. Surface Reconstructions on GaAs(001). *Surf. Sci. Rep.* **2008**, *63* (7), 295−327.
(29) Richter, W. In-Situ Observation of MOVPE Epitaxial Growth. *Appl. Phys. A: Mater. Sci. Process.* **2002**, *75* (1), 129−140.
(30) Döscher, H.; Hannappel, T. In Situ Reflection Anisotropy Spectroscopy Analysis of Heteroepitaxial GaP Films Grown on Si(100). *J. Appl. Phys.* **2010**, *107* (12), 123523.
(31) Law, D. C.; Sun, Y.; Hicks, R. F. Reflectance Difference Spectroscopy of Gallium Phosphide(001) Surfaces. *J. Appl. Phys.* **2003**, *94* (9), 6175−6180.
(32) Maßmeyer, O.; Sterzer, E.; Nattermann, L.; Stolz, W.; Volz, K. Influence of UDMHy on GaAs (0 0 1) Surface Reconstruction before and during Growth of Ga(NAs) by MOVPE. *Appl. Surf. Sci.* **2018**, *458* (15), 512−516.
(33) Zhang, S. B.; Zunger, A. Surface-Reconstruction-Enhanced Solubility of N, P, As, and Sb in III-V Semiconductors. *Appl. Phys. Lett.* **1997**, *71* (5), 677−679.
(34) Bi, W. G.; Tu, C. W. N Incorporation in GaP and Band Gap Bowing of GaNxP1−x. *Appl. Phys. Lett.* **1996**, *69* (24), 3710−3712.
(35) Lee, P. W.; Omstead, T. R.; McKenna, D. R.; Jensen, K. F. In Situ Mass Spectroscopy and Thermogravimetric Studies of GaAs MOCVD Gas Phase and Surface Reactions. *J. Cryst. Growth* **1987**, *85* (1−2), 165−174.
(36) Yoshida, M.; Watanabe, H.; Uesugi, F. Mass Spectrometric Study of Ga(CH3)3 and Ga(C2H5)3 Decomposition Reaction in H2 and N2. *J. Electrochem. Soc.* **1985**, *132* (3), 677−679.
(37) French, C. L.; Foord, J. S. Reaction Kinetics for the CBE Growth of GaAs from Triethylgallium; Computer Modelling Studies Incorporating Recent Surface Spectroscopic Data. *J. Cryst. Growth* **1992**, *120* (1−4), 63−70.
(38) Murrell, A. J.; Wee, A. T. S.; Fairbrother, D. H.; Singh, N. K.; Foord, J. S.; Davies, G. J.; Andrews, D. A. Surface Chemical Processes in Metal Organic Molecularbeam Epitaxy; Ga Deposition from Triethylgallium on GaAs(100). *J. Appl. Phys.* **1990**, *68* (8), 4053−4063.
(39) Stringfellow, G. B. *Organometallic Vapour Phase Epitaxy: Theory and Practice*, 2nd ed.; Academic Press: 1999.
(40) Stringfellow, G. B. The Importance of Lattice Mismatch in the Growth of GaxIn 1-XP Epitaxial Crystals. *J. Appl. Phys.* **1972**, *43* (8), 3455−3460.
(41) Stringfellow, G. B. Microstructures Produced during the Epitaxial Growth of InGaN Alloys. *J. Cryst. Growth* **2010**, *312* (6), 735−749.
(42) Sanorpim, S.; Katayama, R.; Onabe, K.; Usami, N.; Nakajima, K. Lattice-Latching Effect in Metalorganic Vapor Phase Epitaxy Growth of InGaAsN Film Lattice-Matched to Bulk InGaAs Substrate. *Jpn. J. Appl. Phys.* **2010**, *49* (4), 040202.
(43) Kunert, B.; Volz, K.; Koch, J.; Stolz, W. MOVPE Growth Conditions of the Novel Direct Band Gap, Diluted Nitride Ga(NAsP) Material System Pseudomorphically Strained on GaP-Substrate. *J. Cryst. Growth* **2007**, *298*, 121−125.
(44) Stringfellow, G. B. Development and Current Status of Organometallic Vapor Phase Epitaxy. *J. Cryst. Growth* **2004**, *264* (4), 620−630.
(45) Li, S. H.; Larsen, C. A.; Buchan, N. I.; Stringfellow, G. B. Pyrolysis of Tertiarybutylphosphine. *J. Electron. Mater.* **1989**, *18* (3), 457−464.


https://dx.doi.org/10.1021/acs.organomet.0c00078
*Organometallics* 2020, 39, 1772−1781